Spectrochimica Acta Part A 79 (2011) 348–355

Spectrochimica Acta Part A: Molecular and Biomolecular Spectroscopy

journal homepage: www.elsevier.com/locate/saa

Crystal structure of nonadentate tricompartmental ligand derived from pyridine-2,6-dicarboxylic acid: Spectroscopic, electrochemical and thermal investigations of its transition metal(II) complexes

Ramesh S. Vadavi[a], Rashmi V. Shenoy[a], Dayananda S. Badiger[a], Kalagouda B. Gudasi[a,*], L. Gomathi Devi[b], Munirathinam Nethaji[c]

[a] Department of Chemistry, Karnatak University, Dharwad 580 003, India
[b] Department of Post Graduate Studies in Chemistry, Central College Campus, Ambedkar Veedi, Bangalore University, Bangalore 560 001, India
[c] Department of Inorganic and Physical Chemistry, Indian Institute of Science, Bangalore 560 012, India

ARTICLE INFO

Article history:
Received 3 December 2009
Received in revised form
19 December 2010
Accepted 10 March 2011

Keywords:
Nonadentate ligand
Dihydrazone
Pyridine-2,6-dicarboxylic acid
Transition metal complexes
Single crystal X-ray diffraction

ABSTRACT

The coordinating behavior of a new dihydrazone ligand, 2,6-bis[(3-methoxysalicylidene) hydrazinocarbonyl]pyridine towards manganese(II), cobalt(II), nickel(II), copper(II), zinc(II) and cadmium(II) has been described. The metal complexes were characterized by magnetic moments, conductivity measurements, spectral (IR, NMR, UV–Vis, FAB-Mass and EPR) and thermal studies. The ligand crystallizes in triclinic system, space group P-1, with $\alpha = 98.491(10)^\circ$, $\beta = 110.820(10)^\circ$ and $\gamma = 92.228(10)^\circ$. The cell dimensions are $a = 10.196(7)$ Å, $b = 10.814(7)$ Å, $c = 10.017(7)$ Å, $Z = 2$ and $V = 1117.4(12)$. IR spectral studies reveal the nonadentate behavior of the ligand. All the complexes are neutral in nature and possess six-coordinate geometry around each metal center. The X-band EPR spectra of copper(II) complex at both room temperature and liquid nitrogen temperature showed unresolved broad signals with $g_{iso} = 2.106$. Cyclic voltametric studies of copper(II) complex at different scan rates reveal that all the reaction occurring are irreversible.

1. Introduction

In the recent past, multi functional dihydrazones containing amide, azomethine and phenolic functions in duplicate have attracted a lot of attention, mainly due to their potentiality to yield homo- and hetero-polynuclear complexes [1]. The dihydrazones can act as good precursors for macrocyclic systems having available adjacent, similar or dissimilar coordination compartments, which are potential mono, bi and trinucleating ligands. The polynuclear complexes are of interest in the areas such as multimetallic enzymes, and homogeneous and heterogeneous catalysis [1].

Polynuclear uranyl complexes of bissalicylaldehyde-2,6-dipicolinoyl-hydrazone have been reported by Paolucci et al. [2]. Chen et al. [3] have reported a series of trinuclear copper(II) complexes of 2,6-bis[[5-substituted salicylidine]hydrazinocarbonyl] pyridine and also reported the crystal structure of copper(II) complex of the bissalicylaldehyde-2,6-dipicolinoyl-hydrazone [2]. The crystal structure of the complex reveals the tricompartmental nature of the ligand. However, no structural study is reported for the free dihydrazone derived from pyridine-2,6-dicarboxylic acid.

The ligating diversity of such ligands has prompted us to design and synthesize 2,6-bis[(3-methoxysalicylidene) hydrazinocarbonyl]pyridine [$BMSHCPH_4$] and to study its chelating behavior towards different transition metal ions such as manganese(II), cobalt(II), nickel(II), copper(II), zinc(II) and cadmium(II). It has shown binucleating behavior towards lanthanide(III) ions [4].

2. Experimental

2.1. Materials

Pyridine-2,6-dicarboxylic acid (Spectrochem) and 3-methoxy salicylaldehyde (Fluka) were used without further purification and all other solvents were distilled before use.

2.2. Measurements

Elemental analyses were carried out on a Thermoquest CHN analyzer and metal complexes were analyzed for their metal contents by EDTA titration after decomposition with a mixture of HCl and $HClO_4$ [5]. The chloride content of the complexes was determined as silver chloride gravimetrically after decomposing the complexes with HNO_3 [5]. The IR spectra were recorded on a

* Corresponding author. Tel.: +91 836 2460129/2215286; fax: +91 836 27712275.
E-mail address: kbgudasi@rediffmail.com (K.B. Gudasi).

1386-1425/$ – see front matter © 2011 Elsevier B.V. All rights reserved.
doi:10.1016/j.saa.2011.03.011

Nicolet 170 SX FT-IR spectrometer in the region 4000–400 cm^{-1} using KBr discs. The ^1H NMR spectra were recorded in DMSO-d_6 on Bruker Avance 300 MHz spectrometer. Magnetic susceptibility of the metal complexes were measured at room temperature on a Gouy balance using $Hg[Co(SCN)_4]$ as the calibrant and diamagnetic corrections were made by direct weighing of the ligand for diamagnetic pull. Electronic spectra were recorded on a Carry-Bio-50 spectrophotometer in the range 200–1100 nm. The EPR spectrum of a polycrystalline sample was recorded at room temperature and also at liquid nitrogen temperature on a Varian E-4-X-band spectrometer using TCNE as a "g" marker. Conductance measurements were recorded in DMSO (10^{-3}M) using ELICO-CM-82 conductivity bridge with the cell type CC-01 and cell constant 0.53. Electrochemical measurements were performed at room temperature in DMF using Optoprecission potentiostat. A three electrode assembly comprising a glassy carbon working electrode, a platinum auxillary electrode and a saturated Ag/AgCl electrode were used. The supporting electrolyte was 0.1 M TBAP (tetrabutyl ammonium perchlorate). The sample concentration was 0.002 M. Ferrocene was used as a standard showing the Fe(III)/Fe(II) couple at 0.38 V (versus Ag/AgCl electrode) under similar experimental conditions containing 0.1 M TBAP. TGA–DTA studies were carried out in the temperature range 25–1000 °C using TGA7 analyzer, Perkin Elmer, US with a heating rate of 10 °C per minute in nitrogen atmosphere. FAB mass spectra of the complexes were recorded on a JEOL SX 102/DA-6000 mass spectrometer/data system using Argon/Xenon (6 kV, 10 mA) as the FAB gas.

The crystal structure $BMSHCPH_4$ was determined by single crystal X-ray diffraction with dimensions of 0.35 mm × 0.30 mm × 0.30 mm. Data were collected at Department of Inorganic and Physical Chemistry, Indian Institute of Science, Bangalore on a BRUKER SMART APEX- CCD diffractometer with MoKα radiation (λ = 0.71073 Å) at 293 K and scan mode in the range of $1.91 < \theta < 27.45^\circ$. The structure was solved by direct methods and refined by Full-matrix least squares on F^2. All of the non-hydrogen atoms were refined with anisotropic temperature factors. The calculations were performed with the SHELXTL programme [6]. The crystallographic data (CIF file) of $BMSHCPH_4$ have been deposited at Cambridge Crystallographic Data Center (CCDC), 12 Union Road, Cambridge CBZ 1EZ, UK. Copies of the data can be obtained free of charge by quoting the deposition number 256324.

2.3. Syntheses of ligand and complexes

2.3.1. Synthesis of 2,6-bis[(3-methoxysalicylidene)hydrazinocarbonyl]pyridine [$BMSHCPH_4$] [Scheme 1]

A mixture of pyridine-2,6-dicarboxylic acid (***1***) (1.67 g, 10 mmol) and thionyl chloride (***2***) (10 cm^3) was refluxed for 5 h maintaining anhydrous conditions. Excess thionyl chloride was then removed under reduced pressure and further cooled in ice bath for 15 min to get (***3***). 15 cm^3 of super dry ethanol was added and refluxed for 3 h to obtain 2,6-diethylcarboxylatopyridine (***4***). This was further treated with hydrazine hydrate (***5***) (0.02 mol, 1 cm^3) in absolute ethanol (20 cm^3) and refluxed for 2–3 h to obtain 2,6-bis[hydrazinocarbonyl]pyridine (***6***), which was washed with distilled water and recrystallized from hot water to give colorless silky needles.

Yield : 1.336 g, 80%; m.p.285–286 °C.

2,6-bis[(3-methoxysalicylidene)hydrazinocarbonyl]pyridine (***BMSHCPH4***) was synthesized by the literature method [2] with a slight modification. To a hot suspension of (***6***) (1.95 g, 10 mmol) in absolute ethanol (20 cm^3), a solution of 3-methoxy salicylaldehyde (***7***) (3.04 g, 20 mmol) in the same solvent (20 cm^3) was added, and

Table 1
Analytical, electronic spectral data and magnetic moments of $BMSHCPH_4$ and its complexes.

Compound	Empirical formula	Color	MW	Found (calcd.)[a] %					Λ_M (Ω^{-1} cm^2 mol^{-1})	μ_{eff} (B.M)	λ_{max} (nm)
				C	H	N	M	Cl			
$BMSHCPH_4$	$C_{23}H_{21}N_5O_6H_2O$	White	481.47	57.32 (57.38)	4.71 (4.78)	14.50 (14.55)	–	–	–	Dia	314, 308, 304
$[Mn_3(BMSHCP)(H_2O)_7Cl_2]$	$[Mn_3C_{23}H_{17}N_5O_6 7H_2OCl_2]$	Yellow	821.25	33.59 (33.63)	3.72 (3.78)	8.51 (8.53)	(19.95) (20.06)	8.60 (8.65)	0.50	4.82	–
$[Co_3(BMSHCP)(H_2O)_7Cl_2]$	$[Co_3C_{23}H_{17}N_5O_6 7H_2OCl_2]$	Brown	833.23	33.10 (33.14)	3.68 (3.72)	8.36 (8.41)	(21.15) (21.22)	8.50 (8.53)	0.62	3.72	560, 441
$[Ni_3(BMSHCP)(H_2O)_7Cl_2]$	$[Ni_3C_{23}H_{17}N_5O_6 7H_2OCl_2]$	Green	832.50	33.11 (33.17)	3.69 (3.72)	8.38 (8.41)	(21.11) (21.16)	8.48 (8.53)	0.43	2.23	510, 437, 329
$[Cu_3(BMSHCP)(H_2O)_7Cl_2]$	$[Cu_3C_{23}H_{17}N_5O_6 7H_2OCl_2]$	Green	847.07	32.54 (32.60)	3.62 (3.66)	8.21 (8.26)	22.38 (22.50)	8.34 (8.39)	0.47	1.47	620, 442
$[Zn_3(BMSHCP)(H_2O)_7Cl_2]$	$[Zn_3C_{23}H_{17}N_5O_6 7H_2OCl_2]$	Yellow	852.60	32.33 (32.39)	3.61 (3.64)	8.17 (8.21)	22.95 (23.02)	8.26 (8.33)	0.55	Dia	–
$[Cd_3(BMSHCP)(H_2O)_7Cl_2]$	$[Cd_3C_{23}H_{17}N_5O_6 7H_2OCl_2]$	Yellow	993.66	27.74 (27.79)	3.09 (3.12)	7.02 (7.05)	33.87 (33.95)	7.10 (7.15)	0.71	Dia	–

Dia: diamagnetic.
[a] The values in the parenthesis are calculated ones.

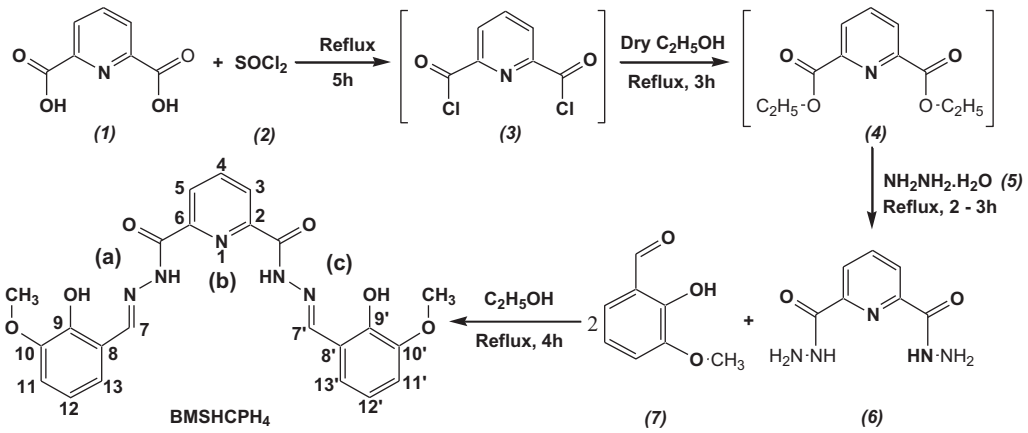

Scheme 1. Synthetic route for $BMSHCPH_4$.

refluxed for 4 h. The yellow microcrystalline product (***BMSHCPH$_4$***) obtained was filtered, washed with hot water followed by hot ethanol, air dried and recrystallized from 2-ethoxyethanol to get crystals suitable for X-ray diffraction studies.

Yield : 1.365 g, 70%; m.p.270–272 °C.

2.3.2. Syntheses of manganese(II), cobalt(II), nickel(II), copper(II), zinc(II) and cadmium(II) complexes [M_3(BMSHCP)·Cl_2·7H_2O]

$BMSHCPH_4$ (0.481 g, 1 mmol) was boiled under reflux with sodium hydroxide (0.080 g, 2 mmol) in 75% aqueous ethanol (10 cm^3) for 30 min. The metal(II) chloride (Mn, Co, Ni, Cu, Zn and Cd) (3 mmol) dissolved in EtOH (10 cm^3) was added and the mixture was refluxed further for 4–5 h. The precipitate obtained was filtered, washed with distilled water and dried in air. Attempts to grow single crystals were unsuccessful.

Yield : 65–76%.

3. Results and discussion

Analytical data are presented in Table 1. All the complexes have 3:1 (M:L) stoichiometry. They are soluble to a limited extent in EtOH, MeOH, DMF and DMSO, but insoluble in H_2O, $CHCl_3$ and C_6H_6. The molar conductance values of the complexes ranging from 0.43 to 0.71 Ohm^{-1} cm^2 mol^{-1} suggest their non-electrolytic nature [7]. The manganese(II), cobalt(II), nickel(II) and copper(II) complexes showed the magnetic moments of 4.82, 3.72, 2.23 and 1.47 B.M. per atom, respectively. These values are less than the high spin metal octahedral complexes probably due to metal-metal interaction in the complexes [8]. Zn(II) and Cd(II) complexes are diamagnetic.

3.1. Crystallographic studies of $BMSHCPH_4$

Crystallographic parameters, selected bond lengths, bond angles and hydrogen bonds in the structure are given in Tables 2–4. The ORTEP [9] and molecular packing diagrams are shown in Figs. 1 and 2, respectively.

Crystal structure of $BMSHCPH_4$ reveals that the whole molecule is coplanar. The plane I [C(1), C(2), C(3), C(4), C(5), C(6), O(1), O(2) and C(23)] make dihedral angles 17.87 (5)° and 33.28 (4)° with the plane II [N(5), C(9), C(10), C(4), C(12) and C(13)] and plane III [C(16), C(17), C(15), C(19), C(20), C(21), O(5), C(6) and C(22)], respectively. The dihedral angle between plane II and plane III is 17.08(5)°. The bond distances and bond angles are in good agreement with the reported ones [10–12]. The conformational designations are

Table 2
Crystal data and structure refinement of $BMSHCPH_4$.

Empirical formula	C23 H23 N5 O7
Formula weight	481.46
Crystal system	Triclinic
Space group	P-1
a (Å)	10.196(7)
b (Å)	10.814(7)
c (Å)	11.017(7)
α (°)	98.491(10)
β (°)	110.820(10)
γ (°)	92.228(10)
V (Å ^{3})	1117.4(12)
Z	2
T (K)	293(2) *K*
Absorption coefficient (mm^{-1})	0.108
λ(MoKα) (Å)	0.71073
F (0 0 0)	504
θ range	1.91–27.45°
Limiting indices	$-13 \le h \le 13$, $-13 \le k \le 13$, $-13 \le l \le 14$
Reflections collected	11906
Independent reflections	4604 [R_{int} = 0.0164]
Data/restraints/parameters	4604/0/408
Goodness-of-fit on F^2	1.052
Final *R* indices [$I > 2\sigma(I)$]	R1 = 0.0467, wR2 = 0.1240

−antiperiplanar across N(4)–C(15) and N(1)–C(7), and *+synperiplanar* across N(3)–C(14) and N(2)–C(8) and the corresponding torsion angles are, −179.71(14)° [N(3)–N(4)–C(15)–C(16)], −176.69(15)° [N(2)–N(1)–C(7)–C(6)], 2.5(2)° [N(4)–N(3)–C(14)–O(4)] and 11.6(3)° [N(1)–N(2)–C(8)–O(3)], and these angles indicate that N(3) and N(2) are in *trans* position to the C(16) and C(6), respectively whereas carbonyl oxygens [O(4) and O(3)] are *cis* to azomethine

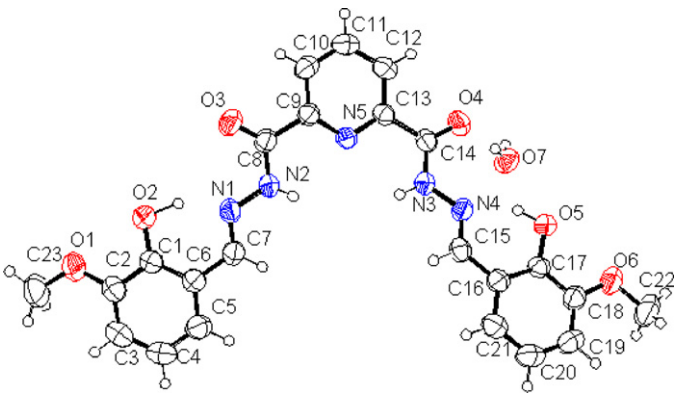

Fig. 1. ORTEP diagram of $BMSHCPH_4$.

Table 3
Selected bond lengths (Å) and angles (°) for $BMSHCPH_4$.

Bond lengths			
O(3)–C(8)	1.220(2)	N(4)–C(15)	1.279(2)
O(4)–C(14)	1.223(2)	N(5)–C(13)	1.333(2)
O(5)–C(17)	1.352(2)	N(5)–C(9)	1.323(2)
O(6)–C(18)	1.361(2)	C(12)–C(13)	1.380(3)
O(6)–C(22)	1.415(3)	C(13)–C(14)	1.491(2)
N(1)–C(7)	1.278(2)	C(15)–C(16)	1.441(2)
N(3)–C(14)	1.338(2)	C(16)–C(17)	1.392(2)
N(3)–N(4)	1.367(2)	C(17)–C(18)	1.396(2)
Bond angles			
C(18)–O(6)–C(22)	117.15(19)	C(17)–C(16)–C(15)	121.31(16)
C(15)–N(4)–N(3)	116.89(15)	C(21)–C(16)–C(15)	119.51(17)
C(9)–N(5)–C(13)	117.30(14)	O(5)–C(17)–C(16)	117.55(16)
O(4)–C(14)–N(3)	124.41(16)	O(5)–C(17)–C(18)	117.55(16)
O(4)–C(14)–C(13)	121.38(16)	O(6)–C(18)–C(19)	125.78(17)
N(3)–C(14)–C(13)	114.20(14)	O(6)–C(18)–C(17)	114.15(16)

nitrogens [N(4) and N(1)]. The torsion angles, N(1)–C(7)–C(6)–C(1) [7.1(3)°], C(7)–C(6)–C(1)–O(2) [−1.1(3)°] and O(2)–C(1)–C(2)–O(1) [0.5(2)°] reveals that N(1), O(2) and O(1) are *cis* to one another and in the similar way O(4), N(4) and O(5) are also in *cis* fashion.

The molecular packing [Fig. 2] shows the existence of intramolecular and intermolecular hydrogen bonds. The distances, O(2)–H(O2)···N(1) and O(5)–H(O5)···N(4) are 2.573 and 2.597 Å. These values indicate the existence of strong intramolecular hydrogen bonding comparable with the earlier report [12].

The oxygen [O(7)] of water molecule in the crystal lattice is intramolecularly hydrogen bonded to carbonyl oxygen, O(4) [O(7)–H(7A)···O(4) = 2.845(3) Å] and intermolecularly hydrogen bonded to O(3) [O(7)–H(7B)···O(3) = 2.874(2) Å] and N(3) [N(3)–H(N3)···O(7) = 3.045(3) Å] of the two different adjacent molecules. Thus water molecule is involved in trifurcate hydrogen bonding.

3.2. IR spectra

The diagnostic IR bands are listed in Table 5. The IR spectrum of $BMSHCPH_4$ showed a series of broad and weak absorption bands extending from 3246 to 2936 cm^{-1} due to intramolecular hydrogen bonding [OH···N=C] [13] and it was confirmed by the crystal studies. In all the complexes, the bands due to ν(OH) and ν(NH) were absent, indicating the complex formation through phenolic oxygen and amide nitrogen via deprotonation [14,15]. The absence of amide I band and presence of a new strong and broad band centered at 1615 cm^{-1} in all the complexes was assigned to the stretching frequency of newly formed C=N–N=C azine moiety indicating the coordination of amide oxygen and nitrogen through enolization and deprotonation [3]. This was further supported by the disappearance of amide II and III bands. The azomethine vibration has shifted to lower wave number in all the complexes by 5–8 cm^{-1} indicating the coordination of azomethine nitrogen to the metal. The band at 1368 cm^{-1} due to ν(C–O), phenolic stretching has shifted to higher wave number by 6–18 cm^{-1} in all the complexes. The 1590 and 1573 cm^{-1} bands of pyridine moiety were not distinctly observed and probably might have merged with the azomethine vibration. The other two vibrations [1461 and 1446 cm^{-1}] have shifted to higher frequency by 6–7 cm^{-1} indicating the coordination of pyridine nitrogen to the metal.

The C–H in plane bend and out of plane bend vibrations showed considerable shift to the higher frequency by 20–22 and 8–12 cm^{-1}, respectively indicating clearly the coordination of pyridine nitrogen to the metal [15].

The presence of a broad band in the region 3434–3470 cm^{-1} was attributed to the ν(O–H) of coordinated water [15]. This was further confirmed by the appearance of a weak non-ligand band in the region 831–856 cm^{-1}, in all the complexes assignable to rocking mode of coordinated water [16]. The presence of coordinated water molecules was further confirmed by TG studies

Looking into the position of coordinating sites in the crystal structure of $BMSHCPH_4$ and bonding sites as suggested by the IR observations, it can be concluded that the ligand behaves as tricompartmental (a, b and c) ligand as shown in Scheme 1.

Table 4
Hydrogen bonds (Å) and angles (°) for $BMSHCPH_4$.

D–H···A	D–H	D···A	H···A	<D–H···A
O2–H2O···O3[a]	1.094(3)	3.934(3)	2.992(3)	144.42(2.07)
O2–H2O···N1[a]	1.094(3)	2.573(2)	1.563(3)	150.63(2.55)
O2–H2O···N2[a]	1.094(3)	3.831(3)	2.751(3)	169.36(2.16)
O5–H5O···N3[a]	0.933(2)	3.871(3)	2.957(2)	166.67(1.92)
O5–H5O···N4[a]	0.933(2)	2.597(2)	1.743(2)	150.81(2.17)
O7–H7A···O4[a]	0.779(2)	2.845(3)	2.071(2)	172.87(2.60)
N3–H3N···O7[b]	0.846(2)	3.045(3)	2.333(2)	142.10(1.74)
C7–H7···O7[b]	0.944(2)	3.401(3)	2.593(2)	143.86(1.60)
N2–H2N···O7[b]	0.813(2)	3.086(3)	2.338(2)	153.17(2.08)
C19-H19···O1[c]	0.965(2)	3.550(3)	2.624(2)	160.84(1.87)
C22–H222···O2[c]	0.993(2)	3.251(4)	2.520(2)	130.25(2.33)
C3–H3···O5[d]	0.947(2)	3.654(4)	2.719(2)	169.40(1.77)
C23H231···O7[d]	0.974(3)	3.729(5)	2.952(3)	137.52(2.48)
O7–H7B···O3[e]	0.821(2)	0.874(2)	2.069(2)	166.52(2.66)

[a] Symmetry transformations used to generate equivalent atoms: *x*, *y*, *z*.
[b] Symmetry transformations used to generate equivalent atoms: *x* + 2, −*y* + 2, −*z*.
[c] Symmetry transformations used to generate equivalent atoms: *x* − 1, +*y* + 1, −*z* + 1.
[d] Symmetry transformations used to generate equivalent atoms: *x*, −*y* − 1, +*z* + 1.
[e] Symmetry transformations used to generate equivalent atoms: *x*, +*y* + 1, +*z*.

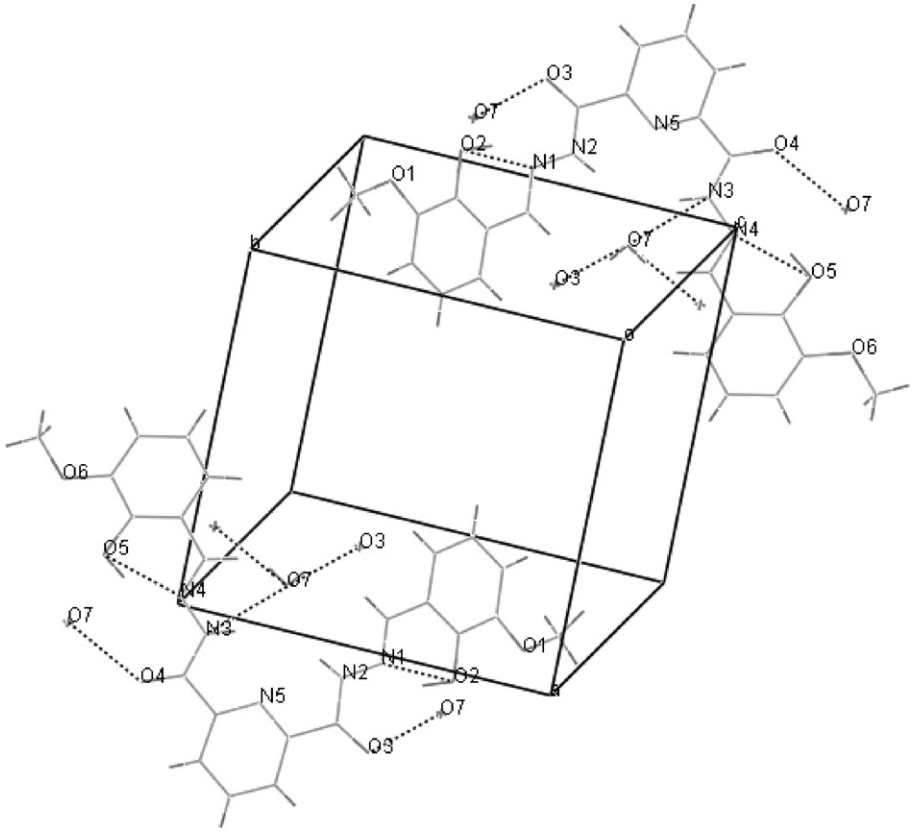

Fig. 2. Molecular packing diagram of BMSHCPH4 showing hydrogen bonds.

3.3. ^1H NMR spectra

The numbering scheme for the assignments of the protons is given in Scheme 1. The ^1H NMR spectrum of $BMSHCPH_4$ in DMSO-d_6 shows only one set of signals indicating the two pendant arms of the pyridine moiety are magnetically equivalent on the corresponding nmr time scale. Two broad singlets at 10.66 and 12.41 ppm are assigned to two NH and two OH protons, respectively [2], and are exchanged by D_2O. The presence of these signals in the downfield region in comparison with aromatic protons was due to the involvement of both the phenolic oxygens and amide nitrogens in intramolecular hydrogen bonding which was confirmed by the crystal structure. A sharp singlet at 8.97 ppm was ascribed to two azomethine protons [H7 and H7′] [2]. A multiplet at 8.30 ppm [H4] and a triplet at 6.91 ppm [H12 and H12′, J = 7.9 Hz] accounts for one and two aromatic protons, respectively. Three doublets at 7.08 [H13 and H13′, J = 7.8 Hz], 7.30 [H11 and H11′, J = 7.6 Hz] and 8.38 ppm [H5 and H3, J = 7.2 Hz] corresponds to six aromatic protons. A sharp singlet in the up field region at 3.85 ppm was attributed to six protons of methoxy group. These assignments have been done by comparing the ^1H NMR of title compound with the 2,6-pyridinedicarboxylic acid and *o*-vanillin [17,18]. In the ^1H NMR spectrum of zinc(II) complex, some of the signals were doubled indicating the magnetically non equivalence nature of the complex in solution. The absence of OH and NH signals clearly indicate the deprotonation during complex formation. The signals due to azomethine protons [H7 and H7′] have been shifted to down field by 0.24 ppm clearly indicating the coordination of azomethine nitrogen to the metal [2]. The signals due to the protons of the pyridine ring [H3, H4 and H5] observed as a broad multiplet in the range from 8.37 to 8.43 ppm suggest the coordination of pyridine nitrogen. The signals due to H12 and H12′, and H11 and H11′ were dou-

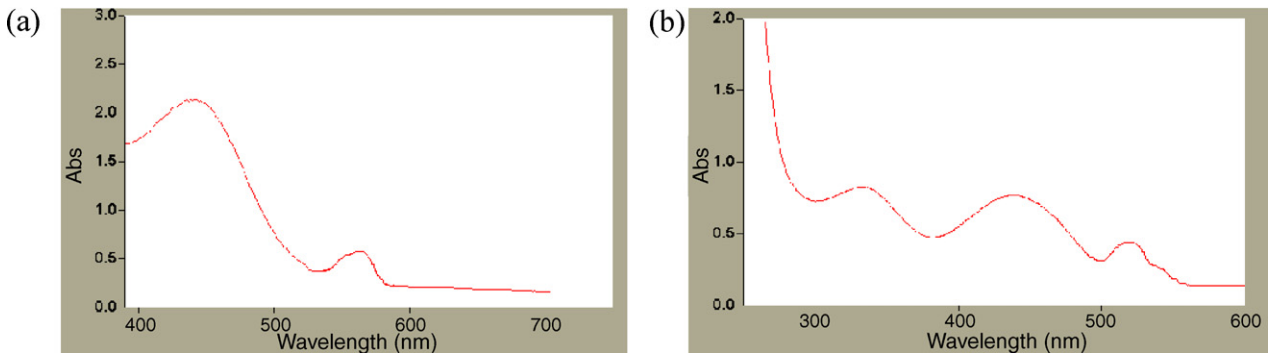

Fig. 3. Electronic spectra of representative complexes; (a) $[Co_3(BMSHCP)(H_2O)_7Cl_2]$, (b) $[Ni_3(BMSHCP)(H_2O)_7Cl_2]$.

Table 5
IR spectral assignments of $BMSHCPH_4$ and its metal complexes (cm^{-1}).

Compound	ν(O–H)	ν(N–H)	ν(C=O)	Amide II	Amide III	ν(C=N)	ν(C=N) of azine	Phen. O–H defor.	Phen. C–O stretch	Py. ring C–C and C–N stretchings	Py. C–H in plane bend	Py. C–H out of plane bend	ν(O–H) water	δ(O–H) water
$BMSHCPH_4$	3246m	3456m	1673s	1541s	1252m	1608m	–	1161s	1368m	1461m	1446w	999m	732s	–	–
$[Mn_3(BMSHCP)(H_2O)_7Cl_2]$	–	–	–	–	–	1607br	1613s	1170w	1372m	1468s	1453w	1022w	745s	3427br	851w
$[Co_3(BMSHCP)(H_2O)_7Cl_2]$	–	–	–	–	–	1607br	1615s	1169w	1374m	1470m	1452m	1019w	744s	3470br	838w
$[Ni_3(BMSHCP)(H_2O)_7Cl_2]$	–	–	–	–	–	1599br	1621s	1168w	1373m	1470m	1455w	1024w	745s	3441br	847w
$[Cu_3(BMSHCP)(H_2O)_7Cl_2]$	–	–	–	–	–	1604br	1610s	1170w	1385m	1470m	1446m	1025w	746s	3434br	856w
$[Zn_3(BMSHCP)(H_2O)_7Cl_2]$	–	–	–	–	–	1600br	1617s	1169w	1375m	1471m	1445m	1025w	746s	3434br	853w
$[Cd_3(BMSHCP)(H_2O)_7Cl_2]$	–	–	–	–	–	1602br	1610s	1169w	1382m	1470m	1470m	1021w	744s	3450br	849m

s: strong; br: broad; w: weak; m: medium.

bled and observed in the up field region at 6.80 and 6.70 and 6.41 and 6.14 ppm. Another signal due to H13 and H13′has also shifted up field by 0.45 ppm. These changes indicate the coordination of phenolic oxygen to the metal [2]. The signal due to methoxy group shifted up field and appeared as two singlets at 3.73 and 3.62 ppm, which clearly supports the non-equivalence of the two pendant arms upon complexation.

3.4. EPR spectra

The EPR spectrum of the present copper(II) complex at room temperature as well as at LNT exhibit unresolved broad signals giving only one 'g' value, i.e., $g_{iso} = 2.106$. Such isotropic spectra, consisting of a broad signal and hence only one g-value, arise from extensive exchange coupling through misalignment of the local molecular axes between different molecules in unit cell (dipolar broadening) and enhanced spin lattice relaxation. This type of spectra unfortunately give no information on the electronic state of the Cu(II) ion present in the complex.

3.5. Electronic spectra

The electronic spectrum of $BMSHCPH_4$ showed three bands in the UV region at 314, 308 and 304 nm. The former two bands were assigned to π–π^* transitions and latter to n–π^* transition. In the electronic spectrum of the cobalt(II) complex [Fig. 3(a)], two spin allowed transitions at 560 and 441 nm were observed, assignable to $^4T_{1g} \rightarrow {}^4A_{2g}(F)$ and $^4T_{1g}(F) \rightarrow {}^4T_{1g}(P)$, indicating an octahedral geometry around the metal center [19,20]. A broad band at 510 nm in the nickel(II) complex [Fig. 3(b)] was due to the $^3A_{2g} \rightarrow {}^3T_{1g}(P)$ transition, indicating an octahedral geometry for the nickel(II) complex [19,21]. In addition to this band, nickel(II) complex showed two broad bands centered at 437 and 329 nm, which are probably due to the charge transfer transitions. A broad band centered at 610 nm, observed as an envelope in copper(II) complex, assigned to the $^2Eg \rightarrow {}^2T_{2g}$ reveals the octahedral geometry [19] and another broad band at 442 nm was due to charge transfer transition. The manganese(II), zinc(II) and cadmium(II) complexes did not show any bands.

3.6. Electrochemistry

The effect of ligands on oxidation-reduction potential and of central metal ion in copper(II) complex, which is a multinuclear cluster, was studied by the cyclic voltammetry. The cyclic voltammograms are scanned at different rates (0.025 V/s, 0.05 V/s and 0.1 V/s) in different potential ranges (+1.2 V to −2.0 V and 1.2 V to −1.6 V).

In general the cyclic voltammograms [Fig. 4] show that all the reaction occurring are irreversible. This irreversibility increases with increase in the sweep rate. Since this system has trinuclear copper, various voltametric peaks appear. The peak at −1.4 V [Fig. 4(b)] is due to the intermediate formed in the reduction reaction, which disappears at high scan rates [Fig. 4(b) and (c)]. The peak at −1.0 V is due to the reduction of Cu^{II} Cu^{II} Cu^{II}–Cu^{I} Cu^{I} Cu^{I} [Fig. 4(a) and (b)]. The peak at −0.6 V [appear only in Fig. 4(a)] is due to the reduction of Cu^{II} Cu^{II} Cu^{II}–Cu^{I} $Cu^{II}Cu^{I}$. This is because; the current continues to be cathodic even when the scan is reversed. The potential is still negative, which is enough to cause reduction. Once the potential becomes positive, reduction of electro active species can no longer occur and the current becomes anodic. The peak at 0.45 V [Fig. 4(b)] corresponds to one electron oxidation of Cu^{II} Cu^{II} Cu^{II}–Cu^{II} Cu^{III} Cu^{II}. This occurs only at higher potential, which is due to satiric effect experienced by central copper. The observed peak shift further apart with increasing scan rates, which further confirms the irreversibility of the system. Moreover the peaks are

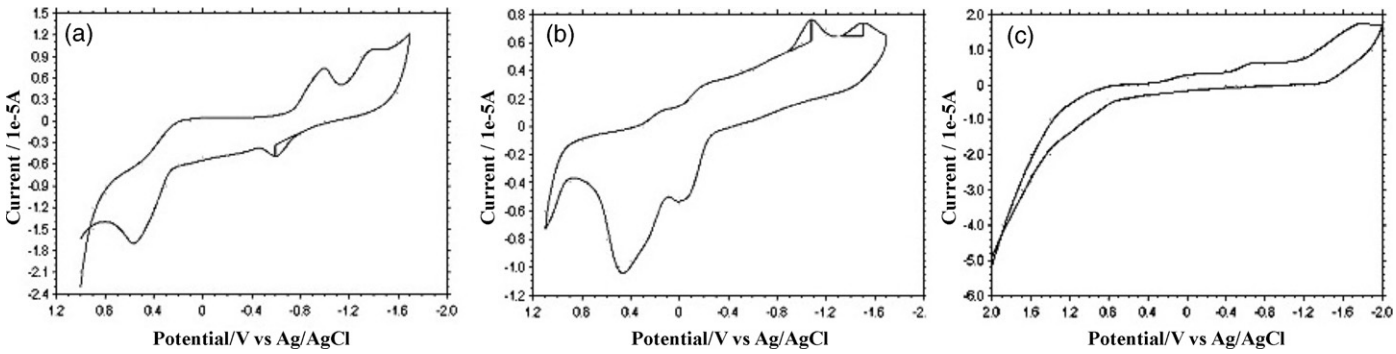

Fig. 4. Cyclic voltammogram of $[Cu_3(BMSHCP)(H_2O)_7Cl_2]$ at different scan rates; (a) 0.05 V/s, (b) 0.025 V/s, (c) 0.1 V/s.

widely separated that no parts of two peaks overlap on the potential axis. Therefore this system can be classified as totally irreversible system. Electrochemical irreversibility is caused by slow electron exchange of redox species with the working electrodes; in this case, at very high scan rate [Fig. 4(c)] since the system is completely irreversible, no oxidation or reduction takes place.

3.7. FAB mass and thermal studies

The FAB mass spectra were obtained for the trinuclear complexes $[Zn_3(BMSHCP)\cdot Cl_2\cdot 7H_2O]$ and $[Cd_3(BMSHCP)\cdot Cl_2\cdot 7H_2O]$. The spectra show the presence of three Zn and three Cd atoms in the complexes with the molecular ion peaks at $m/z = 852$ and 993,

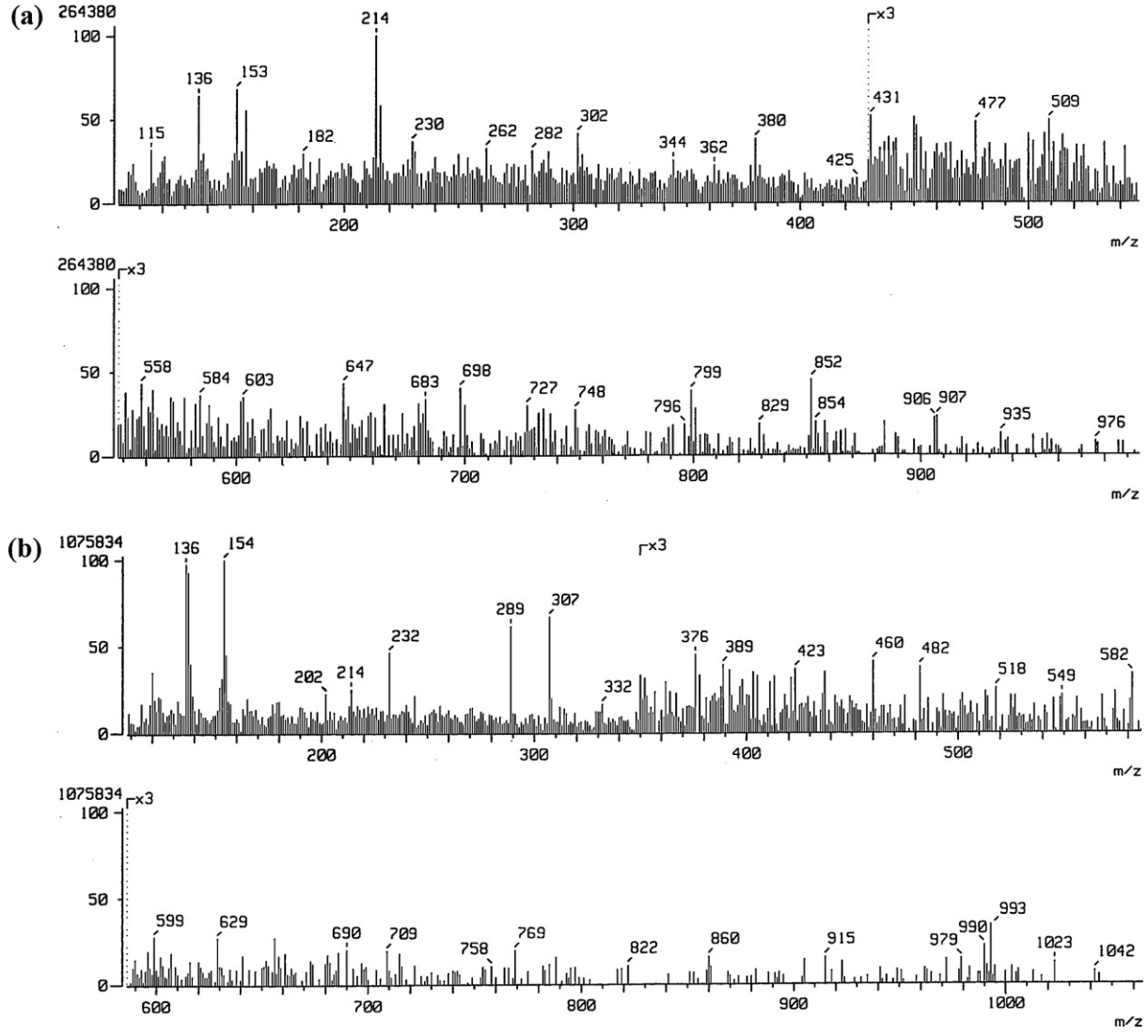

Fig. 5. FAB mass spectra of representative complexes; $[Zn_3(BMSHCP)(H_2O)_7Cl_2]$, (b) $[Cd_3(BMSHCP)(H_2O)_7Cl_2]$.

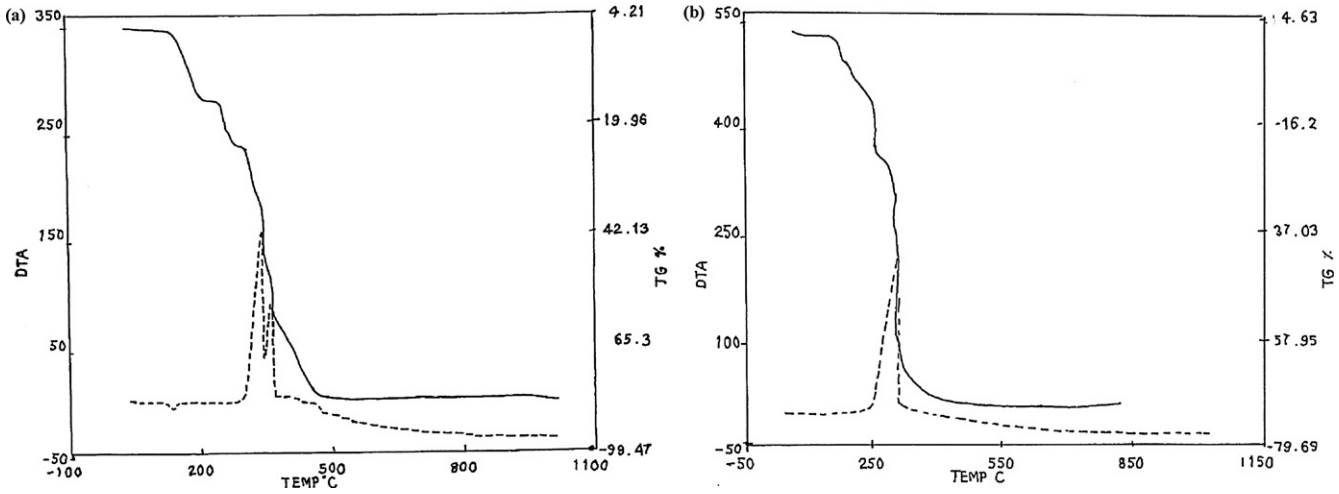

Fig. 6. Thermograms of representative complexes; (a) $[Mn_3(BMSHCP)(H_2O)_7Cl_2]$ (b) $[Cu_3(BMSHCP)(H_2O)_7Cl_2]$.

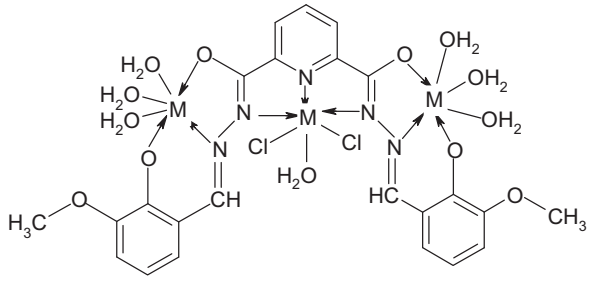

Fig. 7. The proposed structure for all the complexes.

respectively. The *m*/*z* values agreed well with the molecular weight of the species and also confirmed the molecular structure of the complex. Spectra are reproduced in the Fig. 5(a) and (b), respectively.

Thermal study reveals, the manganese(II) and copper(II) complexes decompose in three stages. The manganese(II) complex [Fig. 6(a)] loses a weight of 15.28% (calcd. 15.35%) in the range 140–210 °C and copper(II) complex [Fig. 6(b)] showed a weight loss of 14.80% (calcd. 14.88%) in the range 150–237 °C. The observed weight loss in the first step for both the complexes corresponds to the loss of seven coordinated water molecules. The temperature range rules out the possibility of lattice held water. In the second step two coordinated chlorides were lost in the temperature range 210–320 °C in the manganese(II) complex and the 237–310 °C range in the copper(II) complex, with a mass loss of 8.60% (calcd. 8.65%) and 8.30% (calcd. 8.38%) respectively. In the last step, ligand was lost in the temperature range of 320–490 °C and 310–452 °C with the mass loss of 55.85% (calcd. 55.90%) and 54.15% (calcd. 54.22%) in the manganese(II) and copper(II) complexes, respectively. A plateau is obtained after heating the manganese(II) complex above 490 °C, and copper(II) complex above 452 °C which correspond to the formation of stable MnO and CuO. The weight of MnO and CuO corresponds to 25.95 and 28.12%, respectively and tallies with the metal analysis.

4. Conclusions

The crystal structure of the $BMSHCPH_4$ clearly reveals the presence of donor sites in the tricompartmental mode. From the IR and NMR spectral studies, it is concluded that $BMSHCPH_4$ acts as a nonadentate tricompartmental ligand by coordinating through hydrazonic carbonyl oxygen, hydrazonic nitrogen and phenolic oxygen [in the two side compartments (a and c)] and through pyridyl nitrogen and two hydrazonic nitrogens [in the central compartment (b)] as shown in the Scheme 1. The proposed structure for the all the complexes is depicted in Fig. 7.

Acknowledgements

Thanks are due to S.I.F., I.I.Sc., Bangalore, I.I.T Bombay, C.D.R.I Lucknow and U.S.I.C. Karnatak University, Dharwad for recording NMR, EPR and UV–vis spectra. Authors are thankful to Prof. S.B. Padhye, University of Pune, India for magnetic measurement facilities.

Appendix A. Supplementary data

Supplementary data associated with this article can be found, in the online version, at doi:10.1016/j.saa.2011.03.011.

References

[1] R.A. Lal, S. Adhikari, A. Pal, A.N. Siva, A. Kumar, J. Chem. Res. (S) (1997) 122–123.
[2] G. Paolucci, S. Stelluto, S. Sitran, Inorg. Chim. Acta 110 (1985) 19–23.
[3] X. Chen, S. Zhan, C. Hu, Q. Meng, Y. Liu, J. Chem. Soc. Dalton Trans. (1997) 245–250.
[4] K.B. Gudasi, R.V. Shenoy, R.S. Vadavi, M.S. Patil, S.A. Patil, J. Inclus. Phenom. Macrocycl. Chem. 55 (2006) 93–101.
[5] A.I. Vogel, A Text Book of Quantitative Inorganic Analysis, 3rd Ed., ELBS, 1961.
[6] G.M. Sheldrick, SHELXL 97 Programme for the Solution of Crystal Structures, University of Gottingen, Germany, 1997.
[7] W.J. Geary, Coord. Chem. Rev. 7 (1971) 81–122.
[8] D.L. Arora, K. Lal, S.P. Gupta, S.K. Sahni, Polyhedron 5 (1986) 1499–1501.
[9] C.K. Johnson, ORTEP-I Report, Oak Ridge National Laboratory, Oak Ridge, Tennessee, U.S., 1965, ORNL-3794.
[10] V.C. Tellez, B.S. Gaytan, S. Bernes, E.G. Vergara, Acta Cryst. C58 (2002) o228–o230.
[11] B. Iwasaki, I. Tanaka, A. Aihara, Acta Cryst. B32 (1976) 1264–1266.
[12] S. Francis, P.T. Muthiah, G. Venkatachalam, R. Ramesh, Acta Cryst. E49 (2003) o1045–o1047.
[13] L.J. Bellamy, Infra-red Spectra of Complex Molecules, 3rd Ed., John Wiley and Sons, New York, 1975.
[14] V.B. Rana, S.K. Sahni, S.K. Sangal, J. Inorg. Nucl. Chem. 41 (1979) 1498–1500.
[15] T.F. Zafiropoulos, J.C. Plakatouras, S.P. Perlepes, Polyhedron 10 (1991) 2405–2415.
[16] K. Nakamoto, Infra-red and Raman Spectra of Complex Inorganic and Coordination Compounds, Part B, 5th Ed., Wiley and Sons, Inc., 1997.
[17] SDBS web: http://www.aist.go.jp/RIODB/SDBS (31-10-2004); SDBS No. 2225 HSP-49-058.
[18] SDBS web: http://www.aist.go.jp/RIODB/SDBS (31-10-2004); SDBS No. 2329 HSP-01-166.
[19] N. Raman, S. Ravichandran, C. Thangaraja, J. Chem. Sci. 116 (2004) 215–219.
[20] A.B.P. Lever, Inorganic Electronic Spectroscopy, Elsevier Publishing Company, 1968.
[21] D.N. Sathyanarayana, Electronic Absorption Spectroscopy and Related Techniques, Universities Press (India) Ltd, 2001.